Journal of Cleaner Production 445 (2024) 141390

Contents lists available at ScienceDirect

Journal of Cleaner Production

journal homepage: www.elsevier.com/locate/jclepro

Life cycle assessment of lattice structures: Balancing mass saving and productivity

Giulia Colombini [a], Roberto Rosa [b], Anna Maria Ferrari [b], Silvio Defanti [a,*], Elena Bassoli [a]

[a] University of Modena and Reggio Emilia, Department of Engineering "Enzo Ferrari", Via Pietro Vivarelli, 10, 41125, Modena, Italy
[b] University of Modena and Reggio Emilia, Department of Sciences and Methods for Engineering, Via Giovanni Amendola, 2, 42122, Reggio Emilia, Italy

ARTICLE INFO

Handling Editor: Maria Teresa Moreira

Keywords:
Additive manufacturing
Laser-powder bed fusion
Life cycle assessment
Lattice structures
Productivity
alsi10mg

ABSTRACT

Additive Manufacturing has revolutionized manufacturing processes, offering design flexibility and advances in various applications. The integration of lattice structures into lightweight designs has attracted attention due to their ability to optimize properties such as stiffness, strength and energy absorption. This paper explores the trade-off between mass reduction and productivity while evaluating the environmental sustainability of lattice structures manufactured with Laser-based powder bed fusion for metals Using Life Cycle Assessment, two design variants for an automotive component are compared: a topologically optimized version with a solid bulk section, and a second design with lattice structures for additional weight reduction. Experimental measurements and a detailed analysis of the laser strategy were performed to build the Life Cycle Assessment inventory. The integration of lattice structures allowed a weight reduction of 6 %, but resulted in a significant decrease in productivity and a higher environmental impact. Surprisingly, lattice geometries, often perceived as green solutions, can have negative sustainability implications due to longer manufacturing times and impact of auxiliary equipment. Successful implementation of environmentally sustainable designs requires a balance between mass reduction and productivity while addressing potential environmental consequences.

1. Introduction

Additive Manufacturing (AM) is a new set of manufacturing technologies, capable of creating three-dimensional objects starting from a digital model by joining together consecutive layers of material. Unlike subtractive technologies, these processes have enabled and ensured numerous design advantages. They offer greater design freedom and significant improvements, such as reduced component count in assemblies, creation of pre-assembled structures and optimized design studies for complex geometries, which has established the technology in a wide range of applications (Moreno Nieto and Moreno Sánchez, 2021).

The design capabilities offered by AM techniques have facilitated the development and integration of innovative geometric architectures, such as lattice structures, into the design of lightweight components. Lattice structures are topologically ordered, three-dimensional, open-cell structures consisting of one or more recurring unit cells described by a series of beam elements or struts connected at nodes (Zadpoor, 2019), or by the periodic arrangement of 3D surfaces (Defanti et al., 2024). This remarkable constructive solution allows the construction of components with optimized properties by tuning the structural features of the lattice elements, such as unit cell size or geometric configurations (Boursier Niutta et al., 2022). The use of reticular structures is particularly advantageous for the design of lightweight parts while maintaining or even improving fundamental properties such as stiffness, strength and energy absorption (Boursier Niutta et al., 2022). The high possibility to tailor their properties makes lattice structures versatile for various industries, from biomedical to aerospace and automotive.

Despite the remarkable freedom of design enabled by AM, lattice reticula stretch the boundaries of what is feasible, especially in the case of Laser Based Powder Bed Fusion of metals (Vilardell et al., 2019). The manufactured reticulum can be quite different from the nominal one, in terms of accuracy but also of defects (Sola et al., 2020a). Particularly in the downskin areas, the presence of cracks and dross affects the failure modes and the energy absorption efficiency (Mantovani et al., 2021). In-depth experimental characterization is needed to tune FE models and relate the effective mechanical response to the direction-specific assessment of the accuracy and microstructural integrity (Erturk et al., 2022).

In the study by Kulangara et al. (2021), the use of lattice structures is evaluated for the design optimization of a brake pedal manufactured by

* Corresponding author. University of Modena and Reggio Emilia, Department of Engineering "Enzo Ferrari", via Pietro Vivarelli, 10, 41125, Modena, Italy.
E-mail address: silvio.defanti@unimore.it (S. Defanti).

https://doi.org/10.1016/j.jclepro.2024.141390
Received 3 October 2023; Received in revised form 25 January 2024; Accepted 20 February 2024
Available online 21 February 2024

the Powder Bed Fusion process, using a laser based system (PBF-LB/M). Specifically, a honeycomb lattice structure characterized by a cell size of 12 mm × 8 mm with a strut thickness of 2 mm–8 mm is implemented in the component. Through the comparative finite element (FE) analysis of the performances of the initial component and its optimized version, it is found that by introducing the lattice structure, a reduction of 21.2% in the mass of the component can be achieved, with equal performance for the load case studied. Moreover, in Aslan et al. (Aslan and Yıldız, 2020), the design of a suspension arm is optimized by integrating three different lattice structures in a portion of the component geometry. The results demonstrate that the implementation of such structures can lead to a reduction in mass of up to 10.9 % compared to the starting model, while ensuring a stress value below the limit imposed by the material and simultaneously improving the strength of the component. Mantovani et al. (2022) evaluate different methodologies for the topology optimization of a steering column support. In particular, subsequent AM-oriented topology optimizations of the geometry are performed, by comparing the results of a using bulk material only, with those achieved by a combination of bulk material and graded lattice structures. A weight reduction of 38.6% was achieved compared to the original solid design, by using tetrahedral beam-based lattice structures to interpret intermediate density resulting from topology optimization. The result is enabled by adopting a reduced penalty factor so that intermediate relative densities are calculated (Campo et al., 2019). Similar achievements are obtained by Izri et al. (2022) in the case of a hip implant, where Weaire-Phelan lattice elements enable mass reductions between 19 and 57 % for a shell thickness that goes from 1 down to 0.2 mm.

AM technologies, which are characterized by the selective deposition or consolidation of specific portions of material, are generally defined as "green" technologies when compared to traditional manufacturing methods, due to the little scrap fraction, low energy requirements, and generally lower consumption of resources, also in comparison to the geometric complexity of the parts that can be produced with such technology (Torres-Carrillo et al., 2020; Paris et al., 2016; Cappucci et al., 2020; Liao et al., 2023). With a view to improving the industrial sustainability, i.e. developing and manufacturing goods using a cost-effective technological system that minimizes environmental impact by saving energy and resources, different design solutions are made feasible by the adoption of AM processes. In particular, the application of lattice structures is widely considered as an environmentally sustainable design choice, as it leads to components with lower mass thereby reducing the processed material volume, and the required build energy (Dani et al., 2020). However, assessing the environmental impact of AM requires consideration of total primary energy consumption, which depends on the equipment but also on the specific build strategies and process parameters used in component fabrication (Faludi et al., 2017). Such an approach requires the combined knowledge of environmental assessment methods and of detailed construction mechanisms adopted in AM.

This study aims therefore to perform a comparative analysis of the primary resources involved in manufacturing a component in its solid form and with the integration of lattice structures, in order to quantify the differences in terms of productivity and environmental sustainability of the two design choices. The assessment focuses specifically on the production of a metal component using Powder Bed Fusion laser-based technology (PBF-LB/M) (ASTM INTERNATIONAL and International Organization for Standardization, 2021).

The environmental impact of the two designs is comparatively assessed using the Life Cycle Assessment (LCA) methodology. This modelling framework computes the potential environmental impacts across the complete life cycle of a product, process, service, or system (Hellweg and Milà i Canals, 2014).

2. Materials and methods

2.1. Analysis of the PBF-LB/M process

Unlike the majority of literature studies (Cappucci et al., 2020; Dani et al., 2020; Priarone et al., 2018; Böckin and Tillman, 2019), which only consider the build phase, this work adopts a more comprehensive approach based on the concept of unit process life cycle inventory (UPLCI) (Ramirez-Cedillo et al., 2021). The method analyses the PBF-LB/M process through its three distinct phases that are repeated cyclically for each job (Fig. 1a) and identifies the resources (inputs) and the outputs. In each unit process, the LCI measured variables are electrical energy, inert gas consumption, raw powder, and waste (Fig. 1b). Each step is evaluated individually in terms of energy consumption and resource utilization based on the production of components made from the AlSi10Mg alloy using the SLM 280 dual laser machine (SLM Solution GmbH, Lübeck, Germany). The machine specifications are reported in Table 1.

The delineation of system boundaries (as depicted in Fig. 1c) is specifically defined to encompass solely the operational phases of the PBF-LB machine, excluding ancillary activities like maintenance, machine cleaning, and powder disposal. Moreover, this delineation aims to isolate the operation of the machine from external influences originating from other facets of the manufacturing process, such as material handling and post-processing.

The first phase is the pre-processing, which includes all the preparatory actions required to bring the machine into the ideal condition for the actual melting phase. It consists of several important operations, which are carried out in the following order: sieving of the powder recycled from previous jobs to exclude agglomerated or oxidized particles; then installing the build platform in the work chamber, followed by "zeroing" it to align its top with the bottom of the build chamber; and heating it to a predefined temperature. The preheating temperature depends on the material and is optimized to reduce the temperature gradient between the platform and the first consolidated layers. In the case considered, it was 150 °C. At the end of these actions performed by the operator, the working chamber is purged of oxygen and filled with an atmosphere of inert gas, in this case argon, to ensure an oxygen content of less than 0.1%, as required for the printing process.

Once all the aforementioned steps have been completed, the actual consolidation process begins. The time required to complete this step varies mainly according to the size and shape of the component. To this regard, this study aims at overcoming the common estimate of build time as a function of the mass of built material, by considering that the same amount of material with different spatial distribution turns into different scanning strategies. Consequently, a more detailed assessment of the build time can be achieved. During the execution of the main task in this phase, i.e. laser activity, auxiliary electrical devices are activated simultaneously to maintain optimal working conditions for the laser. A recirculation pump integrated into the machine continuously feeds argon into the build chamber at a constant speed of 22 m/s throughout the printing process to avoid potential defects related to the formation of a metal vapor plume and the ejection of droplets from the melt pool (spatters). Additionally, a chiller is also activated to keep the temperature of the laser at about 19 °C.

During the third phase, or post-processing stage, both the component and the platform are cooled in the machine before the working chamber is opened. Once a temperature suitable for the operator is reached, depowdering is performed, where the remaining unmelted powder is collected and stored for reuse in subsequent jobs (Denti et al., 2019). The entire chamber and the tools used in it, such as the recoater, are cleaned to remove the remaining powder particles. Usually, the finished component undergoes further processes, such as stress-relieving treatments, cutting from the build plate, removal of supports, heat and surface treatments. However, these processes are beyond the scope of this analysis, which focuses on a cradle-to-gate analysis of the PBF-LB/M

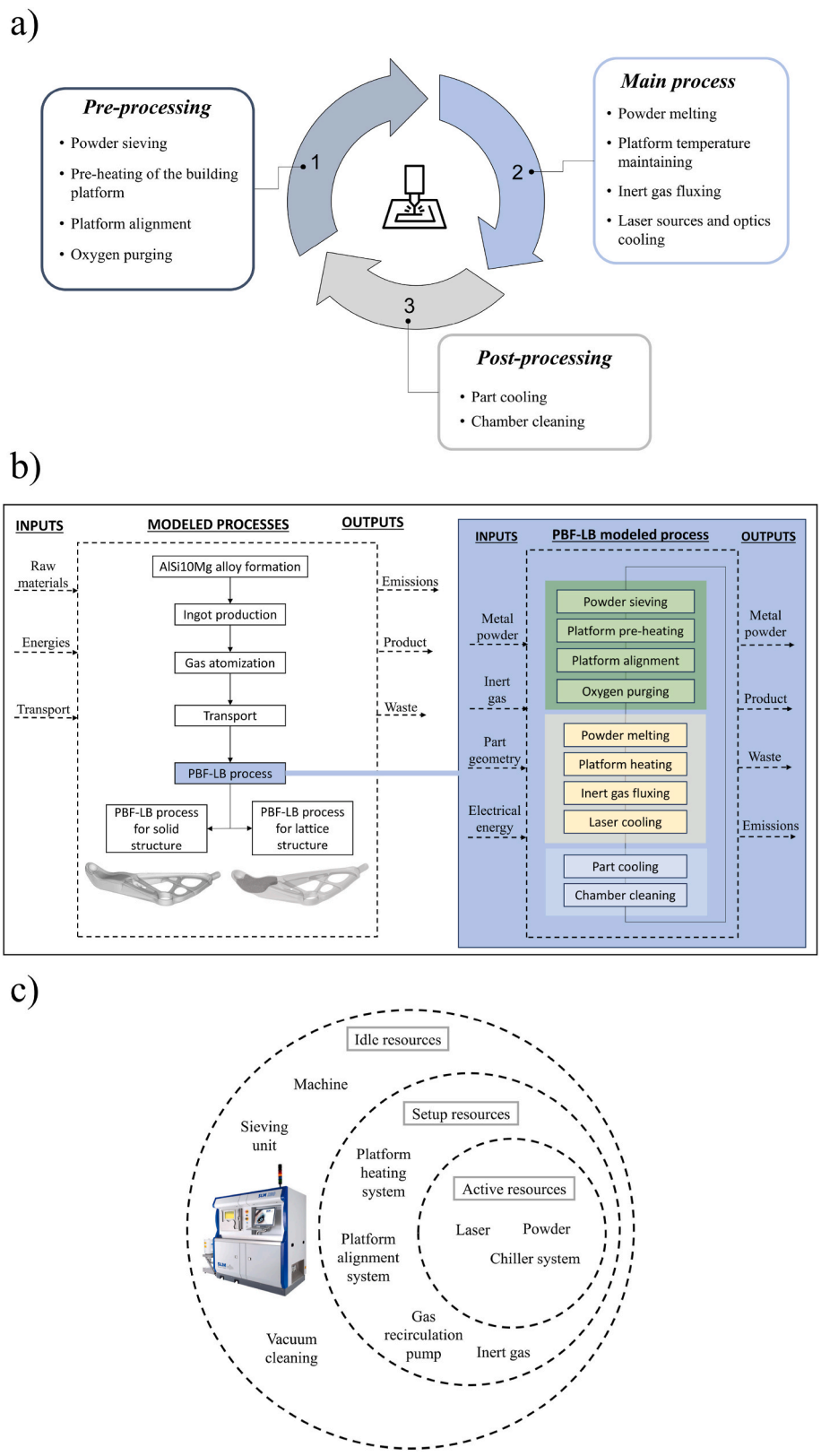

Fig. 1. a) Schematic illustration of the three phases in the PBF-LB/M process, b) LCI data and unit process diagram for the PBF-LB/M process, c) System boundaries.

process itself.

Therefore, the processes and associated equipment investigated in this study are listed in Table 2.

Among the equipment mentioned, only the cooling, sieving, and final vacuum cleaning units are separate from the main machine. The L-PBF apparatus includes a workstation with various tools and devices integrated into its structure. Therefore, some operations attributed to the SLM280 machine are actually performed by the integrated equipment. In this study, the melting operation by the laser and the powder distribution by the recoater are classified as the main manufacturing

Table 1
Specifications of the SLM 280 machine used for the experimental activities.

Machine type	SLM 280 dual laser
Maximum build envelope (X Y x Z)	280 × 280 × 365 mm
Laser power	2 × 400W Yb-Fiber-Laser
Working pressure in chamber (overpressure)	11.5–12.5 mbar
Power supply	400 V 3NPE, 63 A, 50/60 Hz, 3.5–5.5 kW
Chilled water connection	From chiller
Average Argon consumption during construction	5 l/min
Average Argon consumption in the purging phase	110 l/min
Compressed air requirement	ISO 8573–1:2010 [1:4:1] 7 bar

Table 2
List of the actions and devices considered in the cradle-to-gate analysis of the PBF-LB/M technology.

	Action	Device
Pre-processing phase	Powder sieving	PSM 100 unit
	Pre-heating of the building platform	SLM 280 printing machine
	Platform alignment	SLM 280 printing machine
	Oxygen purging and inert gas fluxing	Recirculation pump
Main processing phase	Powder melting	SLM 280 printing machine
	Maintaining platform heating temperature	SLM 280 printing machine
	Inert gas fluxing	Recirculation pump
	Laser source and optics cooling	Chiller unit
Post-processing phase	Part cooling	SLM 280 printing machine
	Chamber cleaning	Industrial vacuum cleaner

activities, while all the others are considered auxiliary to production.

2.2. Data inventory following in-depth UPLCI methodology

The described process analysis is essential for the definition of the characteristic input and output flows, according to the UPLCI methodology and reported in Fig. 1 a) and 1 b). The main input resources involved in the evaluated manufacturing process are identified as the electrical energy needed to run the machine and auxiliary devices, the metal powder produced by gas atomization and the argon gas used to protect the molten metal from oxidation. The corresponding output resources, in addition to the final manufactured part, are the emissions and waste resulting from the process. According to the in-depth approach of UPLCI methodology for LCI data inventory collection (Kellens et al., 2012), field surveys and experimental measurements were conducted during the production of a test job, which allowed the evaluation of the activation sequence, the power consumption and the duration of the activity intervals. Specifically, the experimental data used in this study relate exclusively to the production of AlSi10Mg alloy components made with the SLM 280 dual laser machine. While the detailed process analysis leading to the inventory of the actions and devices involved is of general validity, the setting parameters and resulting consumptions are specific to the raw material selected. For example, the flow rate delivered by the recirculation pump, the heating temperature of the platform and, of course, the energy required by the laser to melt the powder are material-dependent.

2.2.1. Electrical consumption

To estimate electricity consumption, the power and current values of the appliances under consideration were measured over time during a test job. For the devices that are separate from the machine, such as the chiller and the sieve, the current values were measured directly with individual ammeters throughout the three process phases of Fig. 1.

For the PBF-LB/M machine itself and the integrated auxiliary systems, instead, the power meter was connected to the main electrical panel. The measured power corresponds to the overall consumption of the machinery. Fig. 2 presents the absorbed power in idle, setup, and building phase, following the UPLCI schematic methodology (Ramirez-Cedillo et al., 2021). The graph reports the variation of the electrical power absorbed by the SLM280 machine during the test job and includes the identification of the start and completion of each specific task during the construction. Therefore, in order to determine the net power values associated with each integrated device, it was necessary to perform subtraction operations between the different contributions. The results of the calculation, together with the measurements collected for the individual devices, are listed in Table 3.

2.2.2. Time measurement

During the series of experiments described in section 1.2.1, the exact duration of the individual process steps was also determined. As already mentioned, the selected material has a direct influence on the preparatory and final process steps and thus on the time intervals required for the configuration of the machine. The consistent durations of the individual actions in the pre- and post-processing phases are listed in Table 3.

The duration of laser activity in the fabrication of a metal component is closely related to: i) the geometric characteristics of the part, i.e. its overall volume and height, and ii) the building strategy and specific laser parameters, tuned to achieve high density, excellent surface finish, high mechanical response. In this analysis, the implemented laser strategy is commonly referred to as the contour-core strategy (Hellweg and Milà i Canals, 2014; Priarone et al., 2018). At each slice, the inner region, called core, does not require special accuracy and detail resolution and is therefore usually scanned with increased laser speed and power to increase productivity; the outer section, which follows the perimeter of the part and is called contour, is consolidated with the opposite strategy, i.e. with lower laser speed and power, to ensure accuracy and surface quality. An additional set of parameters is used to create support structures. In this study, support structures are only consolidated every two layers, which reduces the building time and facilitates support removal. All process parameters adopted for the present study are compiled in Table 4.

2.2.3. Raw materials

The main raw material for PBF-LB/M technology is metal powder produced by the gas atomization process. The initial amount of powder is loaded into the tank located at the top of the central body of the machine, and is distributed by the recoater throughout the process. At each layer, a small excess of powder goes into the overflow container. This powder, together with the unmelted powder surrounding the part at the end of the job is sieved and recycled for subsequent jobs. It is common to recycle between 90 and 98% of the overall powder needed to run a job but not used to build the part. The remaining scrap percentage consists of agglomerates and oxidized particles. Recycling ratio was set at 96% for this study. Argon is also needed as a resource: it is continuously flooded into the chamber during the preparatory purging phase, and then in smaller quantities throughout the build phase. The inventory for these resources, obtained both from experimental investigation and the SLM 280 machine data sheet, are listed in Table 5.

2.3. Case study

After collecting key data, the method was applied to a case study consisting of an aluminum automotive component, namely the lower arm of a MacPherson front strut suspension system, whose original

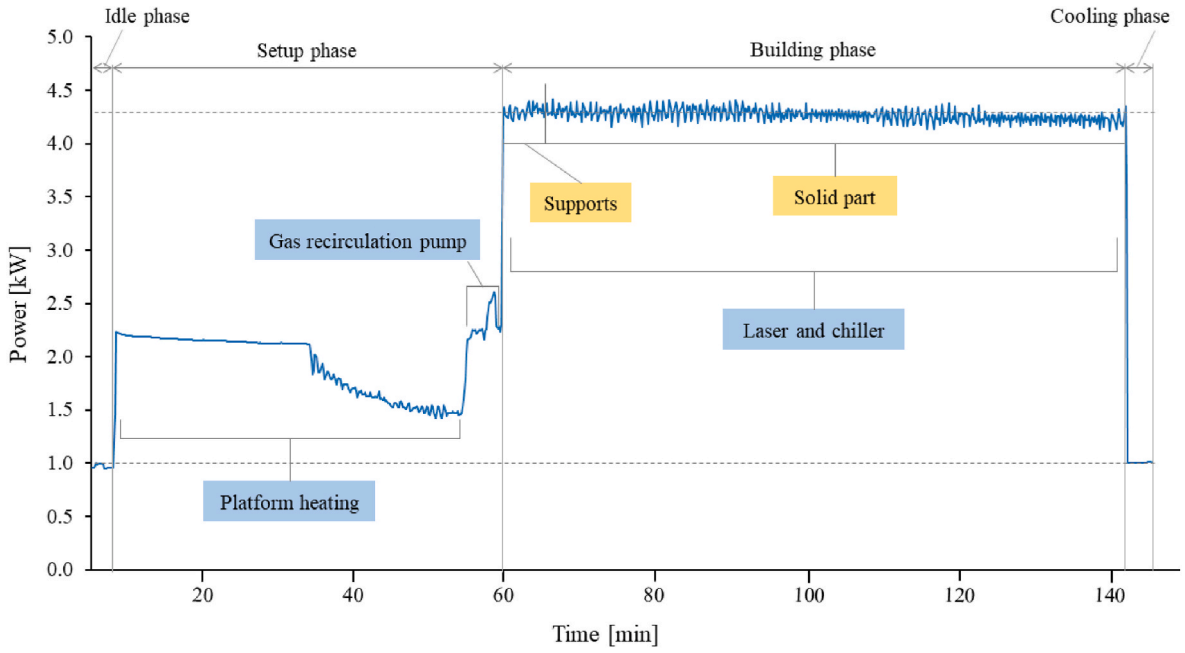

Fig. 2. Power absorption measured during the test job of the PBF-LB/M system with integrated auxiliary devices.

Table 3
Electrical power evaluated during field measurements in the different steps of a PBF-LB/M job and time required to complete setup and post-processing operations. Duration of the main processing phase is not specified because it depends on the components to be built.

	Action	Electrical power [kW]	Duration [h]
Pre-processing phase	SLM280 machine idle condition	0.95	–
	Operation of PSM 100 sieving unit	0.20	0.50
	Heating of the building platform to 150 °C	1.13	0.58
	Platform alignment	0.54	0.17
	Chamber purging by the recirculation pump (47% of max. power)	0.64	0.10
Main processing phase	Operation of the recirculation pump during the build (50.5% of max. power)	0.69	Part specific
	Laser melting of the supports	1.25	Part specific
	Laser melting of the part	1.23	Part specific
	Maintaining building platform temperature	0.42	Part specific
	Chiller operation for laser source and optics cooling	1.93	Part specific
Post-processing phase	Part cooling	1.00	1.00
	Vacuum cleaning of the chamber	2.20	2.50

Table 4
Process parameters for AlSi10Mg in this study.

	Process parameters	
	Recoating time	8 s
	Layer thickness	0.05 mm
	Laser scan strategy	Stripes
Core region	Laser power	350 W
	Laser scan speed	1150 mm/s
	Hatch spacing	0.17 mm
Contour region	Laser power	300 W
	Laser scan speed	600 mm/s
Support structures	Laser power	350 W
	Laser scan speed	900 mm/s

Table 5
Inventory of resources.

AlSi10Mg powder	Density	2.67 g/cm^3
	Apparent density	1.46 g/cm^3
	Powder collected in the overflow during the processing phase	300 g/h
	Generic particle size distribution	25–70 μm
	Powder recycling ratio	96%
Argon gas	Density (at 1 atm)	1.784 kg/m^3
	Argon flux during chamber purging (at 1 atm)	110 l/min
	Argon flux during the main processing phase (at 1 atm)	5 l/min

geometry was topologically optimized using the SIMP method (Mantovani et al., 2022) to reduce the mass with a given stiffness constraint (equal to the non-optimized component). Two versions of the part were compared, a first version, resulting from the initial topological optimization of the component, with solid volume and maximum thickness of about 5–6 mm (Fig. 3a), hereafter called "bulk" version, and a second variant that was further lightweighted by the integration of a lattice structure in a defined volume of the previously optimized geometry, covering approximately 15% of the total volume of the component (Fig. 3b). The optimization approach was the same described fully in (Mantovani et al., 2022) and (Campo et al., 2019).

The FE analysis was performed for both versions for 4 load cases: acceleration, braking, right turn, left turn. Specific constraints were applied to simulate the kinematic connections with the chassis.

The bulk version moderately overperformed the stiffness requirements, so in a second step an area was identified where lattice structures were integrated using the Optistruct lattice optimization process. The result was a lighter version of the arm that met the stiffness targets with slightly less abundance. The virtual simulation validated both component designs as viable alternatives that equally met the

Fig. 3. Case study in the bulk (a) and lattice (b) versions. Box dimensions 253 × 154 × 329 mm.

requirements within the accepted deviation of structural behaviour that can result from the optimization process. Therefore, each design was considered as the functional unit for the LCA.

FE validation was tuned through specific experimental measurements of the mechanical response of lattice structures, where microstructural defects arising from the PBF-LB/M process modify the nominal behaviour.

The occurrence of defects, such as cracks on the horizontal beams and uneven beam diameter, has been studied in detail in previous contributions (Mantovani et al., 2021; Sola et al., 2020b).

The lattice-integrated part includes a tetrahedral reticulum with a cell size of 3 mm and a beam diameter varying in the range 0.24–0.4 mm indicated in the darker grey area in Fig. 3b, leading to a mass reduction of 6%.

The aim of the study was to compare the resources involved in the manufacture of the two versions of the component by PBF-LB/M with AlSi10Mg alloy. Along with the environmental impact, a parallel analysis of productivity was also carried out. The component was industrialized using the software Materialise Magics 25 (Materialise Software, Leuven, Belgium). The positioning and orientation were chosen to ensure the component to fit within the overall dimensions of the working chamber, while minimizing the volume of the required support structures. The supports, which were automatically generated by the software taking into account a self-supporting downskin angle of 42° (ASTM International, 2019), were then optimized to avoid intersections, reduce their impact on the part surfaces and to minimize their volume. To ensure that the comparative analysis was as accurate as possible, the same industrialization concept was replicated for the lattice version of the component. In this case, a preparatory step was needed to reduce the number of triangles in the STL file with the "Triangle reduction" tool. By setting a tolerance of 0.5 mm, a maximum angle of 4° and 10 iterations, the number of triangles of the lattice variant was cut from 19 to 8.6 million. The adoption of procedures to reduce file size is imperative when dealing with lattice structures, to avoid extreme computational loads that might be severe bottlenecks or even inhibit the feasibility of reticular geometries (Zhang et al., 2021). The result of the industrialization is shown in Fig. 4 and specified in Table 6. The total volume of supports for the lattice version refers only to the external supports, as those generated automatically by the software inside the lattice portion have been properly deleted, as their removal would have been impossible. Previous studies prove the self-supporting capabilities of the considered structure (Mantovani et al., 2021; Sola et al., 2020b; Bassoli et al., 2023).

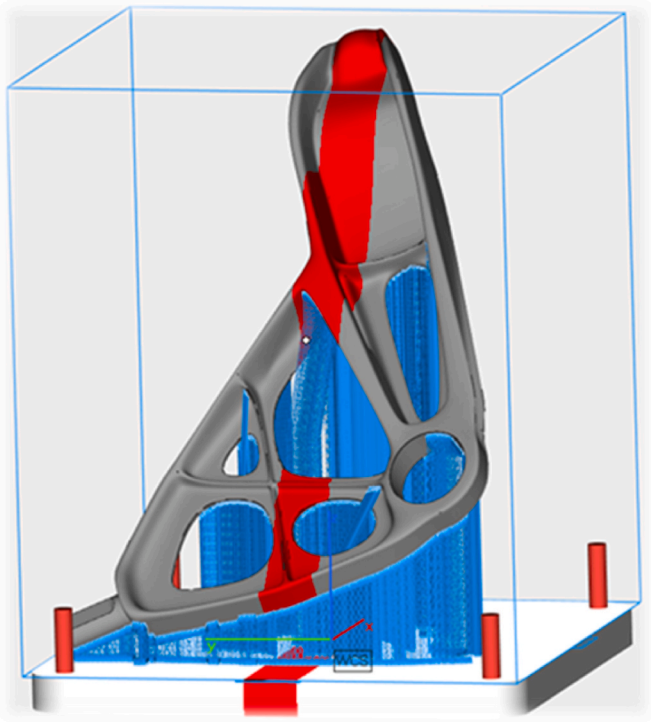

Fig. 4. Job preparation in Materialise Magics of the bulk version of the component.

Table 6
Results of the industrialization of the two components.

	Bulk version	Lattice version
Number of manufactured parts	1	1
Component volume	287.20 mm^3	270.80 mm^3
Mass per part	0.77 kg	0.72 kg
Component surface	106.50 mm^2	381.50 mm^2
Supports volume	55.40 mm^3	54.40 mm^3
Supports mass	0.15 kg	0.15 kg
Component height	320.00 mm	320.00 mm
Number of layers	6396	6394
Lattice volume	–	42.08 mm^3
Total fused mass	0.92 kg	0.87 kg

3. Results and discussion

The time required to produce the two components was calculated using data provided by the SLM 280 machine software: this study has shown that this method of assessment is currently the most reliable, as the projection provided by the Build Processor module in Materialise Magics often provides inaccurate estimates of the actual manufacturing times. It was therefore necessary to generate the. slm file of both parts, including the scan strategies and process parameters defined for the construction, and then load these files into the machine to obtain the actual job duration. The bulk and lattice versions of the part differ greatly in terms of scanning strategy. While the bulk version is consolidated with the above-mentioned contour-core strategy, the second version uses a pure contour consolidation strategy in the lattice area. Therefore, for the production of such components in an SLM280 machine with an AlSi10Mg alloy and a layer thickness of 50 μm, the values given in Table 7 were determined.

The times in the first row refer only to the main processing phase, which consists of the laser time and the recoating time, while pre- and post-processing times are included in the computation of the total job duration. The integration of the lattice structure leads to a loss in

Table 7
Time needed to build the two components.

	Bulk version	Lattice version
Building time	20 h 19 min	29 h 6 min
Total job duration	24 h 40 min	33 h 28 min

productivity of 36%. The resource consumption for the production of the parts was then evaluated, by combining the quantities measured in Section 1.2 with the part-specific values assessed in section 1.3. Table 8 lists the electrical energy calculated from the experimentally determined power of the different devices evaluated over the duration of each action.

The initial mass of powder needed to build a part is calculated as the sum of the amount of powder required to completely cover the finished component, spread by the recoater at each layer, and the additional material that accumulates in the overflow tank during the process. In particular, the first term is calculated considering a volume equal to the area of the build platform multiplied by the value of the z-height of the built component. The value is then multiplied by the apparent density of the AlSi10Mg powder. On the other hand, the excess powder mass that accumulates in the overflow containers is obtained directly by multiplying the overflow rate (Table 5) by the total recoating time during the construction of the component, which in turn is the product of the time for each recoating pass and the number of layers. Since the two geometries were industrialized and thought to be manufactured in the same way, i.e. positioned and oriented to have the same maximum height and number of layers and consequently the same recoating time, the powder mass required was estimated to be equivalent for both geometries. As mentioned before, it is important to emphasise that of this initial mass, most remains as unmelted powder and can be recycled in subsequent jobs: for this case study, a recycling ratio of 96% is assumed (Table 5).

The total argon consumption was estimated using the average flow per hour required (Table 5) for the part's construction time. The consumption in this case is different for the two geometries as they are characterized by different building times. The calculated consumption for the raw materials is shown in Table 9.

The two geometries exhibit different masses: 0.77 kg for the bulk component and 0.72 kg for the component optimized by integrating the lattice structure. Consequently, the second design solution leads to a 6 % reduction in mass. However, this weight reduction is accompanied by an increase in production time and resource consumption. Specifically, the printing time for the optimized component shows a significant increase (+43%) compared to the original geometry. This rise in printing time is primarily due to the scanning strategy associated with the lattice geometry, which leads to the generation of small consolidation regions that are occasionally almost point-like and distributed over the entire part section, as shown in Fig. 5a and b, causing a more complex laser melt path and leading to a longer production time.

Table 9
Total raw materials consumption for the production of the bulk and lattice versions.

	Bulk version	Lattice version
Total initial powder [kg]	41.00	41.00
Overflow powder [kg]	4.26	4.26
Powder recycling ratio	96%	96%
Recycled powder [kg]	38.48	38.52
Total waste powder [kg]	1.60	1.60
Argon for oxygen purging [kg]	1.18	1.18
Argon for building [kg]	10.87	15.58
Total argon consumption [kg]	12.05	16.76

As a result, the extended melting time has a direct impact on the resources consumed during construction, such as electricity and argon. In particular, electrical energy consumption increases (+39%) compared to the full cross-section solution, accompanied by a corresponding increase (+37%) in argon consumption. The initial metal powder requirement remains the same for both solutions. Furthermore, the amount of powder recovered after processing remains the same for both solutions, as the reduction in component mass is not significant enough to affect the quantity. It should be noted that the powder trapped inside the lattice structure was removed through holes specifically designed on the skin of the component. This powder mass was part of the scrap fraction that cannot be recycled.

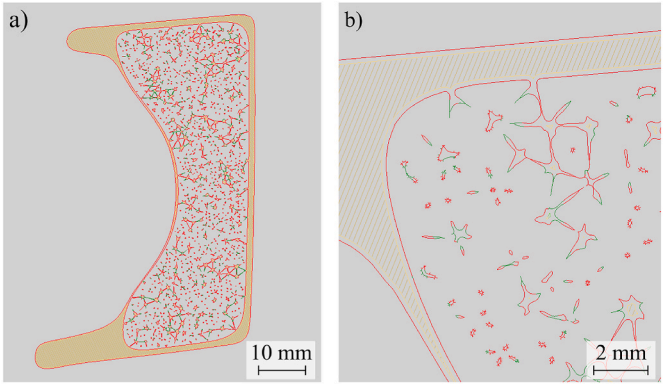

Fig. 5. Laser paths on a slice of the lattice region: a) overall view and (b) detailed view.

Table 8
Total electrical consumption for the production of the bulk and lattice variants of the case study.

Manufacturing phase		Activity	Bulk version			Lattice version		
			Electrical power [kW]	Duration [h]	Electrical energy consumption [kWh]	Electrical power [kW]	Duration [h]	Electrical energy consumption [kWh]
Pre-processing phase		Setup	1.67	1.35	2.25	1.67	1.35	2.25
Main processing phase	Primary action	Laser melting (part + supports)	1.23	20.32	25.07	1.23	29.12	35.92
	Auxiliary action	Maintenance of platform temperature	0.42	20.32	8.49	0.42	29.12	12.17
		Operation of the recirculation pump	0.69	20.32	13.93	0.69	29.12	19.96
		Chiller operation	1.93	20.32	39.25	1.93	29.12	56.25
Post-processing phase		Part cooling (machine idle)	1.00	1.00	1.00	1.00	1.00	1.00
		Cleaning of the chamber	2.20	2.5	5.50	2.20	2.5	5.50
TOTAL					**95.49**			**133.06**

4. Life cycle assessment (LCA)

The Life Cycle Assessment (LCA) phases are detailed hereafter, according to what provided by the ISO 14040–14044 (International Organization for Standardization, 2006a; International Organization for Standardization, 2006b).

4.1. Goal and scope definition

4.1.1. Goal definition

The goal of this LCA study was to quantify and compare the potential environmental impacts associated to two specific geometries designed for the same AlSi10Mg alloy automotive component, utilized as case study, in order to reliably determine the more environmentally sustainable alternative.

4.1.2. System, functional unit, and function of the system

The system that is the subject of this study is the production by the PBF-LB/M additive manufacturing technique of two automotive components, which differ exclusively in the incorporation of a fully bulk structure or a partial lattice structure. The mass of the single component obtained with the two different geometries was selected as the functional unit, which is 0.77 kg for the bulk and 0.72 kg for the lattice version. The function of the studied system, regardless of the geometry (i.e., bulk or lattice), is to be used in the automotive sector as a strut with a certain stiffness.

The system boundaries considered in this study range from the extraction of the raw materials to the production of the powders by gas atomization and their subsequent use for the production of the automotive component by the PBF-LB/M technique, thus allowing an assessment from the cradle to the gate. These boundaries are summarized in the chart in Fig. 1.

All resources used for the production of the components within the system boundaries are schematically represented by the Sankey diagrams in Fig. 6.

4.2. Life cycle inventory (LCI)

Most of the data used in the LCI phase were primary data gathered directly from the experimental activities previously described in Section 2. To effectively model the processes of alloy formation and subsequent atomization, the primary data were integrated with data previously obtained by some of the present authors in the framework of the European Union Horizon 2020 project "Driving up Reliability and Efficiency of Additive Manufacturing" (DREAM) (Sciancalepore et al., 2017), in which the environmental impact associated with the PBF-LB/M technique was studied, exploring different alloys and field applications (Cappucci et al., 2020). The information obtained in the project, particularly on the initial production of raw materials and the machinery required for the different processes, was integrated with the experimental data on the consumption of raw materials and electrical energy previously explained for the two different production strategies employed in the present study. In addition to resource consumption, the study also assessed the environmental impact of the emissions generated in all the phases analyzed. Specifically, the emissions of metal powder and argon that are not retained by the vacuum system in the post-processing phase were calculated, as well as the emissions during the printing phase and their impact on human health and the environment. The study also considered the environmental impact related to the transportation of materials and equipment. For the procurement of metal powder and the SLM machine, a distance of 1500 km was estimated, which corresponds to the distance between the production site in Germany and Italy. For other transfers, a reasonable average distance of 100 km was assumed. The study accounted for road freight transportation using diesel EURO6 lorries with lorry capacities 16–32 metric tons.

The complete inventories for the different life cycle phases that were modelled are detailed in Tables S1–S26 in the Supporting Information section, together with the necessary considerations and assumptions made for their modelling. All inventories were modelled in SimaPro 9.3.0.2 (Pré Sustainability, LE Amersfoort, The Netherlands), using data sets from the Ecoinvent database (EID, version 3.8) (Weidema et al., 2013), following an attributive approach, i.e. through the APOS system model (i.e. allocation at the point of substitution).

4.3. Life cycle impact assessment (LCIA) and interpretation of the LCIA results

The method selected for the life cycle impact assessment (LCIA) was ReCiPe2016. The evaluation was performed first at a midpoint level and then at an endpoint one, with a hierarchical (H) perspective and average weighting set (A) (Huijbregts et al., 2017). The specific evaluation procedure was selected due to its broad acceptance and widespread scientific application, as it allows the evaluation of additional impact categories, compared to alternative methods (Rosa et al., 2022). The environmental impacts of the two different design and production strategies are described at a midpoint level in Table 10. The relative impacts are shown in Fig. 7.

From the results detailed in Table 10 and summarized in Fig. 7 it immediately results evident that the potential environmental impact associated to the integration of lattice structure in the studied automotive component is higher with respect to the case in which the original bulk geometry is implemented, for all the eighteen impact categories considered by the impact assessment method selected (i.e., ReCiPe,

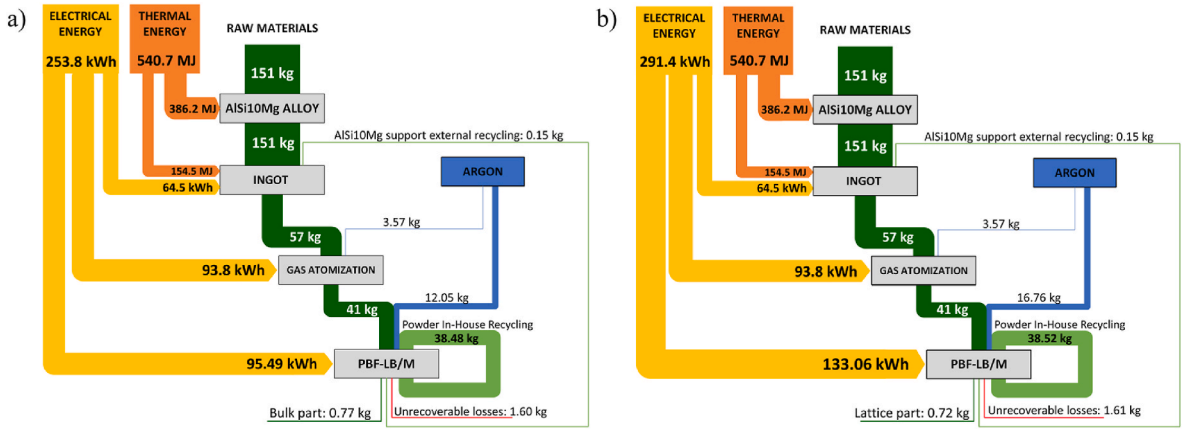

Fig. 6. Sankey diagrams of the flows of energy and materials for: a) bulk version and (b) lattice version.

Table 10
Midpoint environmental impacts (ReCiPe, 2016; H) of 0.77 kg of bulk structure component and 0.72 kg of lattice structure component, both manufactured with L-PBF technology with AlSi10Mg alloy.

Impact category	Unit	Bulk version	Lattice version
Global warming	kg CO2 eq	9.63E+01	1.19E+02
Stratospheric ozone depletion	kg CFC11 eq	6.45E-05	8.06E-05
Ionizing radiation	kBq Co-60 eq	1.82E+01	2.37E+01
Ozone formation, Human health	kg NOx eq	1.90E-01	2.30E-01
Fine particulate matter formation	kg PM2.5 eq	1.38E-01	1.66E-01
Ozone formation, Terrestrial ecosystems	kg NOx eq	1.95E-01	2.36E-01
Terrestrial acidification	kg SO2 eq	3.50E-01	4.26E-01
Freshwater eutrophication	kg P eq	5.28E-02	6.40E-02
Marine eutrophication	kg N eq	4.87E-03	5.83E-03
Terrestrial ecotoxicity	kg 1,4-DCB	5.90E+02	6.22E+02
Freshwater ecotoxicity	kg 1,4-DCB	9.25E+00	1.00E+01
Marine ecotoxicity	kg 1,4-DCB	1.24E+01	1.33E+01
Human carcinogenic toxicity	kg 1,4-DCB	1.40E+01	1.55E+01
Human non-carcinogenic toxicity	kg 1,4-DCB	2.08E+02	2.25E+02
Land use	m2a crop eq	8.37E+00	9.14E+00
Mineral resource scarcity	kg Cu eq	8.20E-01	8.59E-01
Fossil resource scarcity	kg oil eq	2.79E+01	3.47E+01
Water consumption	m^3	2.88E+00	3.62E+00

2016).

The greatest discrepancy is found in the impact category "Ionizing radiation", for which the impact of the lattice version (i.e., 22.5 kBq Co-60 eq) is 30.2% higher than the value determined for the bulk version (i.e., 18.2 kBq Co-60 eq). This is certainly due to the higher amount of electric energy needed in the case of the lattice version. Indeed, in this last scenario (i.e., lattice version) 95.2% of this impact category is due to the emission of Radon-222 to air, which is mainly (97.2%) associated to the dataset "Tailing, from uranium milling {GLO}| treatment of | APOS, U". The latter represents the treatment of residues resulting from the milling of mined uranium ore. This data set refers to the Italian electric energy mix, which is mainly necessary for the production of AlSi10Mg powder. Since the powder is mostly recycled, 48.9% of this dataset is associated to the argon used during the printing phase and 20.2% to the electric energy used to power the auxiliary devices.

As concerns the Global warming impact category, the manufacture of the lattice-based design solution generates 106 kg CO_{2eq}, whose emission in air accounts for 89.6% of the impact. This emission is primarily caused by the EID dataset "Electricity, high voltage {IT}| electricity production, hard coal | APOS, U", according to the Italian electrical energy mix, with 63.5% associated to the electric energy used for auxiliary devices and 25.7% linked to the operation of the laser during the printing process. In the category Stratospheric ozone depletion, the impact associated to the production of the lattice version component is 8.06E-05 kg CFC11 eq. This impact is mainly attributed (for 79.3%) to the emission of dinitrogen monoxide (N2O) in air, accounting for 6.39 E−05 kg CFC11 eq. The process that is mainly responsible for this emission is "Digester sludge {GLO}| treatment of digester sludge, municipal incineration | APOS, U", which is for 55.6% associated to the electric energy used for the auxiliary devices and for 22.5% linked to the functioning of the laser during the printing process. The emission of nitrogen oxides (NO_x) in air affects the two categories of Ozone formation human health and Ozone formation terrestrial ecosystem and is responsible, in the case of the component with the lattice geometry, for 95.7% and 93.3% of the impacts, respectively. These emissions are primarily caused by high voltage electricity production from hard coal, which supplies the electric energy for auxiliary devices and the laser during the printing process. Sulfur dioxide (SO_2) emissions in air mainly contribute to the categories of Fine particulate matter formation and Terrestrial acidification. The process of high voltage electricity production from hard coal is responsible for the majority of these emissions. In the case of the component incorporating the lattice structure, the latter process is associated for 25.7% to the low voltage electricity used during laser operation and for 63.5% to the powering of auxiliary devices (e.g., chiller, recirculation pump).

Freshwater eutrophication is primarily affected by the emission of phosphate into water. In particular, this emission contributes 88.4% to

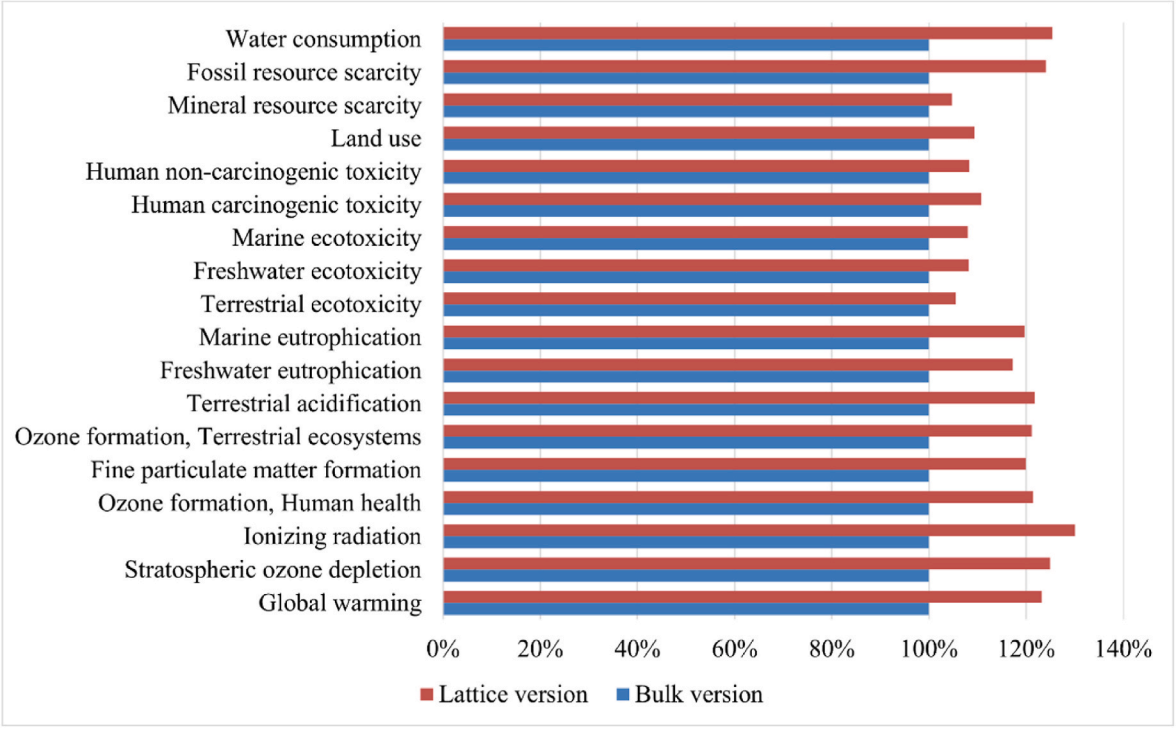

Fig. 7. Relative impacts of the midpoint analysis.

the value of 6.40E-02 kg P eq, which is characteristic of the production of the component with the lattice structure. The Ecoinvent dataset "Spoil from lignite mining {GLO}| treatment of, in surface landfill | APOS, U" contributes significantly (52.1%) to this emission and is 58.8% related to the production of argon consumed during the printing process. Terrestrial ecotoxicity category is mainly influenced by the emission of copper ions into the air. In the case of the lattice geometry, this emission contributes to 68.9% of the total impact of 622 kg of 1,4-DCB. It is primarily caused by brake wear emissions from lorries in connection with the transport of raw materials. The emission of copper ions in water, on the other hand, is responsible for the highest impact in the categories Freshwater and marine ecotoxicity. This water emission is mainly a consequence of the process "Scrap copper {Europe without Switzerland}| treatment of scrap copper, municipal incineration | APOS, U", which in the case of the lattice version of the studied automotive component is ascribed by 43% to powder production (including recycled powder) and by 25.8% to the electrical energy for auxiliary devices. Other categories, such as Human carcinogenic toxicity and non-carcinogenic toxicity, are predominantly impacted by the emission of chromium VI and zinc in water, respectively. Mineral resource and fossil resource scarcity are influenced by the usage of iron and natural gas, respectively. Iron is particularly related to the EID process "Iron ore, crude ore, 46% Fe {GLO}| iron ore mine operation, 46% Fe | APOS, U'', which is used for powder production, while the natural gas consumption is related to the IT electrical energy mix, in particular for the EID process "Natural gas, high pressure {RU}| natural gas production | APOS, U", which is included in the Italian electrical energy mix. The consumption of 422 m^3 of water of natural origin (specifically Water, turbine use, unspecified natural origin IT) represents the main contribution to the Water consumption category in the case of the lattice version of the component. This substance is primarily associated with the Italian electricity mix, which also relies on hydroelectricity sources. However, this process is considered as recovered water as it emits 44.99 m^3 of water per 1 kWh generated.

By performing the endpoint analysis, the damage-oriented results listed in Table S26 in the Supporting Information section are obtained. They can then be categorised into the damage categories considered by the chosen method, namely Human health (expressed in DALY), Ecosystems (expressed in species·yr) and Resources (expressed in USD2013). As expected, the potential endpoint environmental impacts associated with the lattice-based geometry are higher than for the bulk version of the automotive part, regardless of the damage category considered.

In order to facilitate a comprehensive comparison between the two design solutions, their environmental repercussions are quantified and expressed in a single score, represented by eco-indicator points (Pt). The single score serves as a metric for assessing the impact of a specific process and notably, higher values of Pt correspond to more severe environmental impacts. Calculation of Pt involves normalization and weighting operations, which enable a meaningful evaluation of the environmental consequences related to each design solution. The obtained single score results are reported in Fig. 8 and detailed in Table 11.

The single score results clearly demonstrate that the production process involving the lattice structure, despite achieving a reduction in mass, results in an increased (+18%) environmental impact with respect to the original design solution. Specifically, the lattice structure yields a damage of 5.64 Pt, while the original geometry exhibits a comparatively lower environmental impact of 4.79 Pt. Regardless of the geometry considered for the automotive component, the most affected damage category is Human health, contributing in both cases contributes to more than 95% of the total impact expressed in Pt. The impact categories that mainly contribute to this damage category are Fine particulate matter formation and Global warming, Human health, for whose effects sulfur dioxide and carbon dioxide of fossil origin are the main air emissions responsible. These two emissions are mainly associated with the Ecoinvent dataset "Electricity, high voltage {IT}| electricity

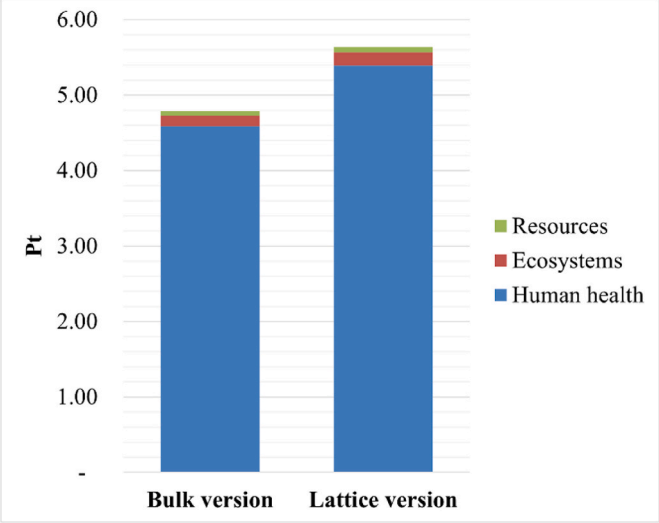

Fig. 8. Eco-indicator points of the two versions of the case study.

Table 11
Eco-indicator points evaluated for the two variants.

Damage category	Unit	Bulk version	Lattice version
Human health	Pt	4.59	5.39
Ecosystems	Pt	0.14	0.17
Resources	Pt	0.06	0.07
Total	Pt	4.79	5.64

production, hard coal | APOS, U", which confirms that the increased electricity demand for the production of the lattice geometry is the main cause of the higher environmental impact. By analysing the single automotive component in which the lattice structure is integrated, it is possible to determine and quantify the role of the different sub-processes for the previously reported single score of 5.64 Pt. These contributions are illustrated in Fig. 9, which shows evidently that the process with the most significant environmental repercussions is the one associated to powder production, followed by the overall amounts of electricity and argon gas employed during PBF-LB/M. Further investigation, in which the production of AlSi10Mg powder is modelled, reveals that the alloy-forming process represents the primary factor contributing to the environmental impact in general. Nonetheless, owing to the characteristic features of the technology, a substantial portion of the raw material can be effectively reused in following jobs, thereby generating an advantageous outcome despite the resultant impact.

Lastly, although this analysis adopts a cradle-to-gate approach, focusing primarily on the production of raw materials and manufacturing technology, it is important to briefly evaluate the potential impact that arises during the use phase of the two different design solutions when implemented in an automotive system. The development of lightweight components leads to a reduction in the overall weight of the assembly and thus to a reduction in energy consumption, expressed in terms of fuel saving during the use phase (Salonitis et al., 2019; Priarone et al., 2023). Nevertheless, as noted by Salonitis et al. (2019), the benefits in the subsequent phase only become visible after a certain vehicle driving distance, defined as the break-even distance, when the design is characterised by a significant consumption of energy and primary resources in the manufacturing phase. These considerations are extended to the present case study, taking into account the implementation in a diesel system. It is found that the lightweight lattice component only surmounts the initial higher impact compared to the bulk solution after 3.5×10^6 km travelled by the vehicle, which is irrelevant for conventional vehicle use. Similar considerations apply to the end-of-life scenario, as the mass saving is too small to provide a

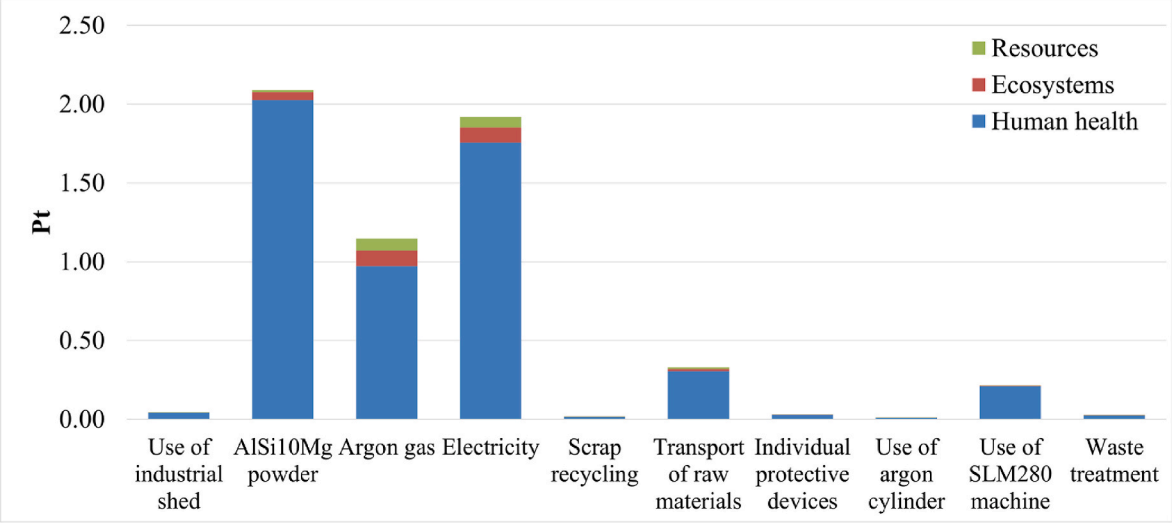

Fig. 9. Single score evaluation details of the lattice version.

significant advantage given the impact of the production phase.

5. Conclusions

The present study aimed to investigate the relationship between design choices for additive manufacturing technologies and the resulting impact on productivity and environmental sustainability. To achieve this, a cradle-to-gate analysis was conducted using the ReCiPe2016 method. Specifically, a comparative analysis was conducted on two design solutions for a component intended for automotive applications: the first design featured a topological optimization and a solid bulk section throughout the whole volume, while the second design was characterized by an additional weight reduction through the integration of lattice structures. The main findings are the following.

- The experimental investigation of the resources required for an PBF-LB/M job showed that the primary contributor to power consumption during processing is due to auxiliary devices operating simultaneously with the laser, such as the laser chiller and the argon recirculation pump.
- The analysis showed that the 6% mass saving enabled by the integration of the lattice structure comes at the expense of a 36% lower productivity. Consequently, electricity and argon consumption also increase significantly in the transition to a lattice-based design.
- The LCA analysis allowed to quantify the result in terms of final damage points, for which the lattice variant of the component is responsible of 5.6 Pt, 0.8 Pt higher than the original bulk geometry. Furthermore, the analyses highlighted that the majority of the emissions characterizing the midpoint analysis were attributable to the significant power consumption throughout the process. Most notably, emissions associated with powder, whose production process has the greatest impact within the cradle to gate cycle, were mitigated due to the significant amount of recycled powder that could be effectively reused in subsequent operations.

The research has shown that lattice geometries, generally touted as green solutions, can instead have a negative impact on sustainability due to longer building times and a high impact of auxiliary devices, which are usually disregarded. In the case of PBF-LB/M, a reduction in the mass of components is not automatically associated with better sustainability. It is essential to take into account how the mass is distributed in the slices, because in mesh-like structures the consolidation of numerous tiny areas has an extremely negative impact on the job duration. For innovative topologically optimized structures, lightweight construction and structural properties must be balanced with productive and environmental aspects.

CRediT authorship contribution statement

Giulia Colombini: Writing – review & editing, Writing – original draft, Software, Investigation. **Roberto Rosa:** Writing – review & editing, Writing – original draft, Software. **Anna Maria Ferrari:** Supervision, Resources. **Silvio Defanti:** Writing – review & editing, Validation, Methodology. **Elena Bassoli:** Writing – review & editing, Writing – original draft, Supervision, Resources.

Declaration of competing interest

The authors declare that they have no known competing financial interests or personal relationships that could have appeared to influence the work reported in this paper.

Data availability

I have shared the link to my data at the attach file step.

Acknowledgements

The authors acknowledge HPE GROUP for their valuable contribution during the experimental phase of this research. This research was funded by Regione Emilia Romagna (Italy), POR-FESR 2014–2020 Actions 1.1.1 and 1.1.4 l.R. 14/2014 grant number E98I17000090009.

Appendix A. Supplementary data

Supplementary data to this article can be found online at https://doi.org/10.1016/j.jclepro.2024.141390.

References

Aslan, B., Yıldız, A.R., 2020. Optimum design of automobile components using lattice structures for additive manufacturing. Mater. Test. 62, 633–639. https://doi.org/10.3139/120.111527.

ASTM International, 2019. ISO/ASTM 52911-1:2019(E) - additive manufacturing — design — Part 1 : laser-based powder bed fusion of metals. ASTM Int 1–15. https://doi.org/10.1520/52911-1-19.2, 2019.

ASTM INTERNATIONAL, International Organization for Standardization, 2021. ISO/ASTM 52900:2021 - Additive Manufacturing - General Principles - Fundamentals and Vocabulary.

Bassoli, E., Mantovani, S., Giacalone, M., Merulla, A., Defanti, S., 2023. On the technological feasibility of additively manufactured self-supporting AlSi10Mg lattice structures. Adv. Eng. Mater. 25, 2201074 https://doi.org/10.1002/adem.202201074.

Böckin, D., Tillman, A.-M., 2019. Environmental assessment of additive manufacturing in the automotive industry. J. Clean. Prod. 226, 977–987. https://doi.org/10.1016/j.jclepro.2019.04.086.

Boursier Niutta, C., Ciardiello, R., Tridello, A., 2022. Experimental and numerical investigation of a lattice structure for energy absorption: application to the design of an automotive crash absorber. Polymers 14, 1116. https://doi.org/10.3390/polym14061116.

Campo, G.A., Vettorello, A., Giacalone, M., 2019. Optimization methodology for continuous heterogeneous structures: a preliminary design of an engine mounting bracket. Key Eng. Mater. 827, 116–121. https://doi.org/10.4028/www.scientific.net/KEM.827.116.

Cappucci, G.M., Pini, M., Neri, P., Marassi, M., Bassoli, E., Ferrari, A.M., 2020. Environmental sustainability of orthopedic devices produced with powder bed fusion. J. Ind. Ecol. 24, 681–694. https://doi.org/10.1111/jiec.12968.

Dani, I., Drossel, W.-G., Milaev, N., Korn, H., Hannemann, C., Hohlfeld, J., Wertheim, R., 2020. Sustainability of industrial components using additive manufacturing and foam materials. Procedia Manuf. 43, 10–17. https://doi.org/10.1016/j.promfg.2020.02.102.

Defanti, S., Giacalone, M., Mantovani, S., Tognoli, E., 2024. Dimensional and Mechanical Assessment of Gyroid Lattices Produced in Aluminum by Laser Powder Bed Fusion, pp. 699–707. https://doi.org/10.1007/978-3-031-44328-2_73.

Denti, L., Sola, A., Defanti, S., Sciancalepore, C., Bondioli, F., 2019. Effect of powder recycling in laser-based powder bed fusion of Ti-6Al-4V. Manuf. Technol. 19, 190–196. https://doi.org/10.21062/ujep/268.2019/a/1213-2489/MT/19/2/190.

Erturk, A.T., Bulduk, M.E., Tarakçi, G., Özer, G., Yarar, E., 2022. Investigation of the microstructure and mechanical characteristics of lattice structures produced by laser powder bed fusion method. Met. Mater. Int. 28, 155–167. https://doi.org/10.1007/s12540-021-01038-y.

Faludi, J., Baumers, M., Maskery, I., Hague, R., 2017. Environmental impacts of selective laser melting: do printer, powder, or power dominate? J. Ind. Ecol. 21 https://doi.org/10.1111/jiec.12528.

Hellweg, S., Milà i Canals, L., 2014. Emerging approaches, challenges and opportunities in life cycle assessment. Science 80 (344), 1109–1113. https://doi.org/10.1126/science.1248361.

Huijbregts, M.A.J., Steinmann, Z.J.N., Elshout, P.M.F., Stam, G., Verones, F., Vieira, M., Zijp, M., Hollander, A., van Zelm, R., 2017. ReCiPe2016: a harmonised life cycle impact assessment method at midpoint and endpoint level. Int. J. Life Cycle Assess. 22, 138–147. https://doi.org/10.1007/s11367-016-1246-y.

International Organization for Standardization, 2006a. ISO 14040:2006 - Environmental Management - Life Cycle Assessment - Principles and Framework.

International Organization for Standardization, 2006b. ISO 14044:2006 - Environmental Management - Life Cycle Assessment - Requirements and Guidelines.

Izri, Z., Bijanzad, A., Torabnia, S., Lazoglu, I., 2022. Silico evaluation of lattice designs for additively manufactured total hip implants, Comput. Biol. Med. 144, 105353 https://doi.org/10.1016/j.compbiomed.2022.105353.

Kellens, K., Dewulf, W., Overcash, M., Hauschild, M.Z., Duflou, J.R., 2012. Methodology for systematic analysis and improvement of manufacturing unit process life-cycle inventory (UPLCI)—CO2PE! initiative (cooperative effort on process emissions in manufacturing). Part 1: methodology description. Int. J. Life Cycle Assess. 17, 69–78. https://doi.org/10.1007/s11367-011-0340-4.

Kulangara, A.J., Rao, C.S.P., Cherian, J., 2021. Topology optimization of lattice structure on a brake pedal. Mater. Today Proc. 47, 5334–5337. https://doi.org/10.1016/j.matpr.2021.06.059.

Liao, J., De Kleine, R., Kim, H.C., Luckey, G., Forsmark, J., Lee, E.C., Cooper, D.R., 2023. Assessing the sustainability of laser powder bed fusion and traditional manufacturing processes using a parametric environmental impact model. Resour. Conserv. Recycl. 198, 107138 https://doi.org/10.1016/j.resconrec.2023.107138.

Mantovani, S., Giacalone, M., Merulla, A., Bassoli, E., Defanti, S., 2021. Effective mechanical properties of AlSi7Mg additively manufactured cubic lattice structures. 3D Print. Addit. Manuf. https://doi.org/10.1089/3dp.2021.0176.

Mantovani, S., Campo, G., Giacalone, M., 2022. Steering column support topology optimization including lattice structure for metal additive manufacturing. Proc. Inst. Mech. Eng. Part C J. Mech. Eng. Sci. 236, 10645–10656. https://doi.org/10.1177/09544062209471 21.

Moreno Nieto, D., Moreno Sánchez, D., 2021. Design for additive manufacturing: tool review and a case study. Appl. Sci. 11, 1571. https://doi.org/10.3390/app11041571.

Paris, H., Mokhtarian, H., Coatanéa, E., Museau, M., Ituarte, I.F., 2016. Comparative environmental impacts of additive and subtractive manufacturing technologies. CIRP Ann 65, 29–32. https://doi.org/10.1016/j.cirp.2016.04.036.

Priarone, P.C., Lunetto, V., Atzeni, E., Salmi, A., 2018. Laser powder bed fusion (L-PBF) additive manufacturing: on the correlation between design choices and process sustainability. Procedia CIRP 78, 85–90. https://doi.org/10.1016/j.procir.2018.09.058.

Priarone, P.C., Catalano, A.R., Settineri, L., 2023. Additive manufacturing for the automotive industry: on the life-cycle environmental implications of material substitution and lightweighting through re-design. Prog. Addit. Manuf. 8, 1229–1240. https://doi.org/10.1007/s40964-023-00395-x.

Ramirez-Cedillo, E., García-López, E., Ruiz-Huerta, L., Rodriguez, C.A., Siller, H.R., 2021. Reusable unit process life cycle inventory (UPLCI) for manufacturing: laser powder bed fusion (L-PBF). Prod. Eng. 15, 701–716. https://doi.org/10.1007/s11740-021-01050-6.

Rosa, R., Pini, M., Cappucci, G.M., Ferrari, A.M., 2022. Principles and indicators for assessing the environmental dimension of sustainability within green and sustainable chemistry. Curr. Opin. Green Sustainable Chem. 37, 100654 https://doi.org/10.1016/j.cogsc.2022.100654.

Salonitis, K., Jolly, M., Pagone, E., Papanikolaou, M., 2019. Life-cycle and energy assessment of automotive component manufacturing: the dilemma between aluminum and cast iron. Energies 12, 2557. https://doi.org/10.3390/en12132557.

Sciancalepore, C., Bondioli, F., Gatto, A., Defanti, S., Denti, L., Bassoli, E., 2017. DREAM: driving up reliability and efficiency of additive manufacturing. In: 2017 IEEE 3rd Int. Forum Res. Technol. Soc. Ind., pp. 1–4. https://doi.org/10.1109/RTSI.2017.8065979. IEEE.

Sola, A., Defanti, S., Mantovani, S., Merulla, A., Denti, L., 2020a. Technological feasibility of lattice materials by laser-based powder bed fusion of A357.0, 3D print. Addit. Manuf. 7, 1–7. https://doi.org/10.1089/3dp.2019.0119.

Sola, A., Defanti, S., Mantovani, S., Merulla, A., Denti, L., 2020b. Technological feasibility of lattice materials by laser-based powder bed fusion of A357.0, 3D print. Addit. Manuf. 7, 1–7. https://doi.org/10.1089/3dp.2019.0119.

Torres-Carrillo, S., Siller, H.R., Vila, C., López, C., Rodríguez, C.A., 2020. Environmental analysis of selective laser melting in the manufacturing of aeronautical turbine blades. J. Clean. Prod. 246, 119068 https://doi.org/10.1016/j.jclepro.2019.119068.

Vilardell, A.M., Takezawa, A., du Plessis, A., Takata, N., Krakhmalev, P., Kobashi, M., Yadroitsava, I., Yadroitsev, I., 2019. Topology optimization and characterization of Ti6Al4V ELI cellular lattice structures by laser powder bed fusion for biomedical applications. Mater. Sci. Eng. 766, 138330 https://doi.org/10.1016/j.msea.2019.138330.

Weidema, B.P., Bauer, C., Hischier, R., Mutel, C., Nemecek, T., Reinhard, J., Vadenbo, C. O., Wernet, G., 2013. Overview and Methodology. Data Quality Guideline for the Ecoinvent Database Version 3. https://ecoinvent.org/wp-content/uploads/2020/10/dataqualityguideline_ecoinvent_3_20130506_.pdf. (Accessed 21 July 2023).

Zadpoor, A.A., 2019. Mechanical performance of additively manufactured meta-biomaterials. Acta Biomater. 85, 41–59. https://doi.org/10.1016/j.actbio.2018.12.038.

Zhang, L., Hu, Z., Wang, M.Y., Feih, S., 2021. Hierarchical sheet triply periodic minimal surface lattices: design, geometric and mechanical performance. Mater. Des. 209, 109931 https://doi.org/10.1016/j.matdes.2021.109931.